

Electron Spin Relaxation Near a Micron-Size Ferromagnet

B. C. Stipe,¹ H. J. Mamin,¹ C. S. Yannoni,¹ T. D. Stowe,² T. W. Kenny,³ and D. Rugar¹

¹IBM Research Division, Almaden Research Center, 650 Harry Road, San Jose, California 95120

²Department of Applied Physics, Stanford University, Stanford, California 94305

³Department of Mechanical Engineering, Stanford University, Stanford, California 94305

(Received 31 August 2001; published 13 December 2001)

Magnetic resonance force microscopy was used to study the behavior of small ensembles of unpaired electron spins in silica near a micrometer-size ferromagnetic tip. Using a cantilever-driven spin manipulation protocol and a magnetic field gradient greater than 10^5 T/m, signals from as few as 100 net spins within a 20 nm thick resonant slice could be studied. A sixfold increase in the spin-lattice relaxation rate was found within 800 nm of the ferromagnet, while no effect due to silica surface proximity was detected. The results are interpreted in terms of Larmor-frequency magnetic field fluctuations emanating from the ferromagnet.

DOI: 10.1103/PhysRevLett.87.277602

PACS numbers: 76.30.-v, 07.55.-w, 85.70.-w

Long spin relaxation times are important for the success of many proposed solid-state quantum computing and spintronic devices [1–4], and for the manipulation and imaging of individual spins by magnetic resonance force microscopy (MRFM) [5,6]. However, spin relaxation and related quantum decoherence effects may be strongly influenced by thermal fluctuations in nearby materials, such as conductors and ferromagnets. Typically, these materials must be present in order to read out the spin state or to locally control the electric or magnetic fields experienced by the spin. In addition, impurities or other defects at surfaces and interfaces may influence spin relaxation. Understanding these relaxation effects will be crucial for a wide variety of future experiments, especially those that rely on microfabricated structures to manipulate small ensembles of spins.

MRFM is a recently developed technique that is suitable for characterizing spin behavior with high sensitivity and nanometer-scale spatial resolution [7–12]. In the present work, we use MRFM with 100 spin sensitivity and 20 nm effective slice thickness to study relaxation effects for a dilute system of paramagnetic electron spins located in close proximity to a micron-size ferromagnetic particle (the MRFM tip). By locally measuring the spin-lattice relaxation time T_1 , the spectral density of magnetic field fluctuations emanating from the ferromagnet can be determined. Furthermore, by taking advantage of the high spatial resolution of MRFM, the relaxation induced by the nearby sample surface can be separately evaluated.

MRFM experiments were performed in vacuum at 3 K using a tip-on-cantilever configuration (Fig. 1). The custom single-crystal silicon cantilever had dimensions of $190 \mu\text{m} \times 3 \mu\text{m} \times 850 \text{nm}$, resulting in a flexural-mode eigenfrequency $f_c = 21.4 \text{kHz}$ and a spring constant $k = 0.014 \text{N/m}$. The cantilever exhibited quality factors ranging from 200 000 to 2000 depending on the tip-to-sample spacing [13]. Cantilever motion was detected with a fiber-optic interferometer operating at 1310 nm wavelength [14]. The sample consisted of

optically polished fused silica (Corning 7943) that had been irradiated by ^{60}Co γ rays to produce silicon dangling bonds (E' centers) with a spin concentration of $\sim 2 \times 10^{18} \text{cm}^{-3}$ [15–17].

The spins were polarized by the inhomogeneous field from the magnetic tip $B_{\text{tip}}(x, y, z)$ in combination with a homogeneous external field B_{ext} supplied by a superconducting magnet. The magnetic tip, which was designed to have large magnetization and strong uniaxial anisotropy, was fabricated by gluing a micron-size particle of $\text{Pr}_2\text{Fe}_{14}\text{B}$ near the end of the cantilever in the presence of an orienting magnetic field. A focused ion beam was then used to mill a flat on the bottom of the particle, resulting in a tip that was roughly cylindrical with diameter $1.25 \mu\text{m}$ and length $1.75 \mu\text{m}$ (Fig. 1b). Cantilever magnetometry [18] was used to determine the total moment ($m_{\text{tip}} = 1.5 \times 10^{-12} \text{J/T}$), anisotropy field ($B_A = \mu_0 H_k = 26 \text{T}$), and coercivity ($\mu_0 H_c = 2.3 \text{T}$). The moment and anisotropy are somewhat less than one would expect based on the bulk properties of single-crystal $\text{Pr}_2\text{Fe}_{14}\text{B}$ at low temperatures [19], possibly because of oxidation or ion beam damage.

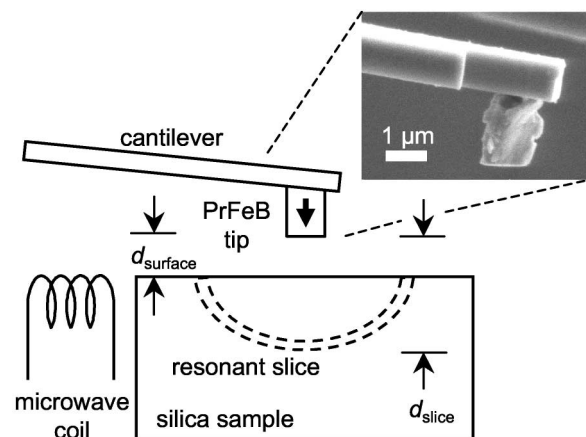


FIG. 1. Schematic diagram of the MRFM setup. Inset shows a scanning electron micrograph of the $\text{Pr}_2\text{Fe}_{14}\text{B}$ particle tip.

Electron spin resonance was excited at 6 GHz using a microwave magnetic field produced by an untuned, 200 μm diameter coil (field strength $B_1 = 0.3$ mT). The inhomogeneity of the tip field confined the magnetic resonance to a narrow slice satisfying the resonance condition $B_0(x, y, z) = \omega_{rf}/\gamma_s$, where B_0 is the total polarizing field (tip field plus external field), ω_{rf} is the frequency of the microwave field, and γ_s is the gyromagnetic ratio of the spin ($\gamma_s/2\pi = 2.8 \times 10^{10}$ Hz/T). At 6 GHz, the resonance condition is $B_0(x, y, z) = 0.214$ T. The axial distance between the tip and the resonant slice, denoted by d_{slice} , was controlled by adjusting B_{ext} (e.g., larger values of B_{ext} move the resonant slice away from the tip).

To probe the spin polarization in the vicinity of the resonant slice, a new spin manipulation and measurement protocol, designated by OSCAR (oscillating cantilever-driven adiabatic reversals), was implemented (Fig. 2a). The cantilever is continuously driven to “self-oscillate” by using the interferometer signal in a gain-controlled positive feedback loop to excite a piezoelectric element located near the cantilever [20]. As a result, the cantilever acts as the frequency determining element of the oscillator so that the cantilever oscillation frequency instantaneously follows its natural frequency, which is determined in part by the back action force exerted by the spins on the magnetic tip. With the cantilever oscillating and the microwave source initially turned off, the spins are allowed to polarize for a

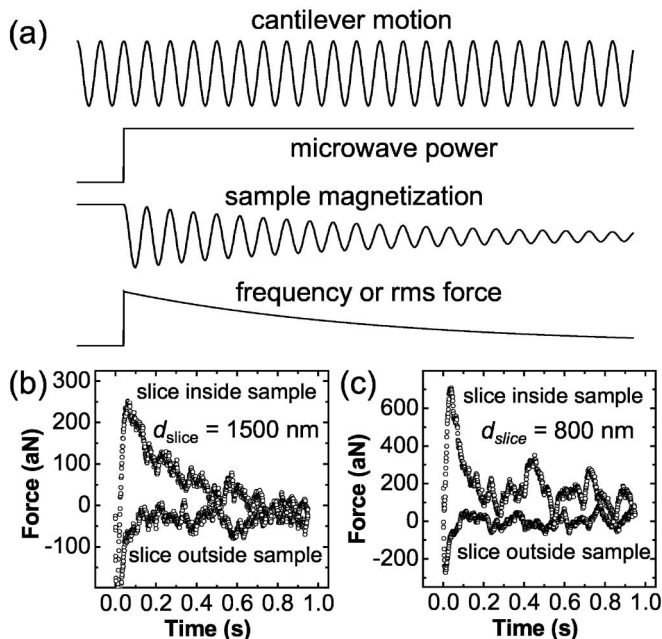


FIG. 2. (a) The OSCAR spin manipulation and detection protocol. In the actual experiment, the oscillating magnetization can persist for several thousand cycles. (b) Spin signal, presented here in terms of rms force, for $B_{\text{ext}} = 184$ mT (corresponding to $d_{\text{slice}} = 1500$ nm). Signal lifetime was $\tau_m \approx 275$ ms. Also shown is the null signal obtained when the slice is outside the sample ($B_{\text{ext}} < B_{\text{onset}}$). (c) Spin signal obtained for $B_{\text{ext}} = 139$ mT (corresponding to $d_{\text{slice}} = 800$ nm). Smaller d_{slice} gives a shorter signal lifetime: $\tau_m \approx 68$ ms.

time longer than the spin-lattice relaxation time. The microwave field is then switched on at a time that is synchronized with the cantilever reaching an extremum of oscillation. As the cantilever vibrates, the position of the resonant slice within the sample also oscillates through a region of the sample, and the spins in that region are cyclically inverted due to the effect of adiabatic rapid passage [17]. The cyclic inversion generates an oscillatory interaction force that effectively modifies the cantilever restoring force, resulting in an apparent change in spring constant $\Delta k \approx F_{\text{spin}}/\Delta z$, where F_{spin} is the rms amplitude of the oscillating force from the spins and Δz is the rms cantilever amplitude (typically 20 nm). The change in spring constant shifts the cantilever oscillation frequency by $\Delta f/f \approx (1/2)(\Delta k/k)$, which is detected by an analog frequency demodulator [20]. This basic detection scheme was typically combined with some additional signal processing in order to eliminate spurious (nonspin) responses [21].

The cantilever vibration amplitude determines the effective thickness of the probed slice, and thus the number of spins contributing to the signal. For small slice penetration depths, $F_{\text{spin}} \approx GN(\mu_B^2 B_0/k_B T)A\Delta z$, where G is the tip field gradient, N is the spin density, T is temperature, A is the area of the slice that has penetrated into the sample, μ_B is the Bohr magneton, and k_B is Boltzmann’s constant. With $\Delta z = 20$ nm, $A = 0.25 \mu\text{m}^2$, and $G = 10^5$ T/m, the slice contains roughly 10^4 spins with net polarization of $\sim 480\mu_B$ and gives $F_{\text{spin}} \approx 450 \times 10^{-18}$ N. With moderate signal averaging (~ 500 averages), polarizations as small as $100\mu_B$ could be studied.

Examples of typical magnetic resonance signals are shown in Figs. 2b and 2c. The signals have peak amplitudes roughly consistent with the above estimate and were found to decay within a fraction of a second. The signals were observed only when B_{ext} was in the range $B_{\text{onset}} < B_{\text{ext}} < 0.22$ T (Fig. 3), where B_{onset} corresponds to the field where the slice is just entering the sample surface. By measuring the dependence of the onset field on tip-to-surface distance d_{surface} , both B_{tip} and the tip field gradient G could be determined. As shown in Fig. 3b, when d_{surface} was changed by 140 nm (from 610 to

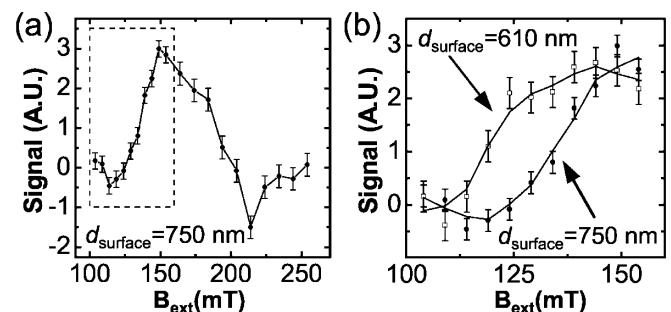


FIG. 3. (a) Signal amplitude as a function of external field for $d_{\text{surface}} = 750$ nm. (b) Detail showing signal onset for $d_{\text{surface}} = 610$ nm and $d_{\text{surface}} = 750$ nm.

750 nm), the onset field shifted by 15 mT, demonstrating an axial field gradient $G = 1.1 \times 10^5 \text{ T/m} = 1.1 \text{ G/nm}$.

The lifetime of the signal is determined by relaxation processes that occur during the cyclic reversals [17]. The associated relaxation time, which we denote as τ_m , depends on many factors, including B_1 strength, adiabatic reversal rate, and spin-lattice relaxation times in both the lab frame (T_1) and the rotating frame ($T_{1\rho}$). In addition to these known dependencies, τ_m was found to be a strong function of tip proximity. As can be seen in Figs. 2b and 2c, τ_m was observed to drop from 275 ms at $d_{\text{slice}} = 1500 \text{ nm}$ to 68 ms at $d_{\text{slice}} = 800 \text{ nm}$. One could argue that this effect is due to the larger field gradient at small d_{slice} , resulting in higher sweep rates (dB_0/dt) and violations of the adiabatic condition. To check this, we reduced Δz to 8 nm, but found no increase in τ_m . Other possible causes include the influence of magnetic noise emanating from the tip or screening of the B_1 field by the tip. Whatever the cause, the decrease in τ_m at close tip proximity could pose a key challenge for future single-spin MRFM experiments, since those experiments will likely operate with $d_{\text{slice}} < 100 \text{ nm}$. For such small values of d_{slice} , one might expect severe reduction in τ_m , necessitating significantly wider detection bandwidth and, therefore, reduced signal-to-noise ratio.

We also measured the spin-lattice relaxation time T_1 , which has a more straightforward physical interpretation than τ_m . To measure T_1 , the spins in the resonant slice were first allowed to polarize for sufficient time, then adiabatically inverted by turning on the microwave field for one-half of a cantilever cycle (Fig. 4a). Then, with the microwave field off, the spins were allowed to recover for a variable period of time before the resulting spin polarization was probed using the OSCAR protocol. The resulting exponential inversion-recovery curve was numerically fitted to determine T_1 (Figs. 4b and 4c).

T_1 was found to systematically decrease from 13 s for $d_{\text{slice}} = 1500 \text{ nm}$ to about 2 s for $d_{\text{slice}} = 800 \text{ nm}$ (Figs. 4b–4d). In contrast, when d_{slice} was kept constant (i.e., B_{ext} constant) and the slice penetration depth varied by physically moving the sample position, T_1 was unchanged (Fig. 4e). We were able to probe penetration depths as small as 50 nm. From these observations, we conclude that it is the magnetic tip, rather than the silica surface, that is responsible for the observed decrease in T_1 at small d_{slice} .

Spin-lattice relaxation is known to be a sensitive probe for magnetic field fluctuations at the Larmor frequency [22]. Near a ferromagnet, possible origins of field fluctuations include thermally driven magnetic moment fluctuations and thermal noise currents. The relaxation rate for spins under the influence of a thermally fluctuating magnetic field is given by [22]

$$\frac{1}{T_1} = \frac{1}{2} \gamma_s^2 [S_{B_x}(\omega_0) + S_{B_y}(\omega_0)], \quad (1)$$

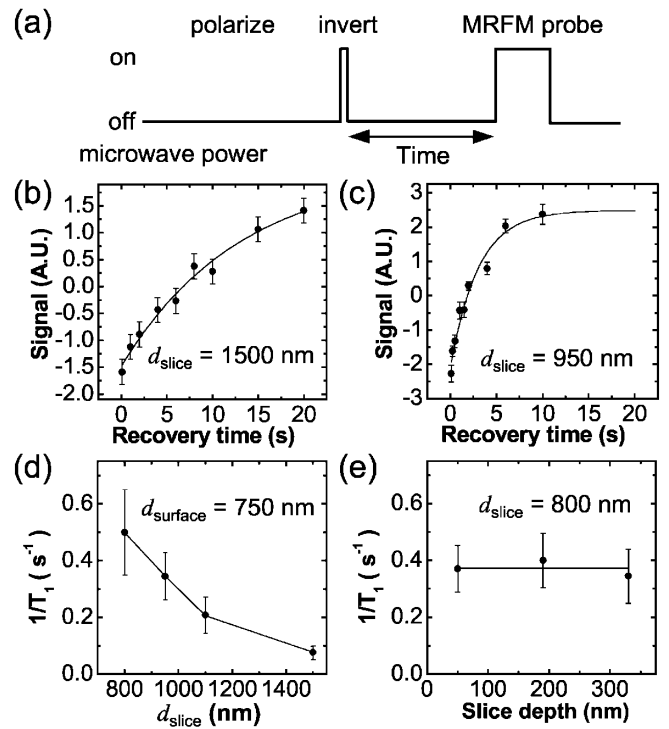


FIG. 4. (a) Timing diagram for T_1 inversion-recovery measurement. (b) Spin polarization as a function of recovery time for $d_{\text{slice}} = 1500 \text{ nm}$ and $d_{\text{surface}} = 750 \text{ nm}$. A fit to the data gives $T_1 = 13.1 \text{ s}$. (c) When d_{slice} is reduced to 950 nm , T_1 drops to 2.9 s . (d) Relaxation rate vs d_{slice} showing substantial increase as the slice approaches the tip. Here $d_{\text{surface}} = 750 \text{ nm}$. (e) Relaxation rate as a function of the depth of the slice below the sample surface. Here, $B_{\text{ext}} = 139 \text{ mT}$ and $d_{\text{slice}} = 800 \text{ nm}$.

where $\omega_0 = \gamma B_0$ is the Larmor frequency. B_x and B_y are the two transverse field components which, for simplicity, are assumed to be uncorrelated with (double-sided) spectral densities given by $S_{B_q}(\omega) = \int_{-\infty}^{\infty} B_q(t)B_q(t + \tau)e^{-i\omega\tau} d\tau$. Assuming the fluctuations in the x and y directions have similar magnitudes such that $S_{B_x}(\omega) = S_{B_y}(\omega)$, Eq. (1) simplifies to $1/T_1 = \gamma^2 S_{B_x}(\omega_0)$. Based on this relation, the field noise corresponding to the shortest observed T_1 of 2 s is $6 \times 10^{-8} \text{ T/Hz}^{1/2}$.

Fluctuations of the tip magnetic moment are one possible source of magnetic field noise [23]. To obtain an analytical estimate of this noise, we model the tip as a single domain particle with large anisotropy and consider fluctuations in the average magnetic moment (i.e., for the uniform mode) at frequencies far below the ferromagnetic resonance (FMR) frequency ($\omega_{\text{FMR}} \approx \gamma_m B_A \approx 2\pi \times 700 \text{ GHz}$ for our tip, where γ_m is the gyromagnetic ratio appropriate for the ferromagnet). Based on the linearized Landau-Lifshitz-Gilbert (LLG) equation and the fluctuation-dissipation theorem, the transverse moment spectral density is white (i.e., frequency independent) and given by $S_{m_x} = 2\alpha m_{\text{tip}} k_B T / \gamma_m B_A^2$, where α is the LLG damping parameter [24].

The transverse moment fluctuations give rise to transverse field fluctuations. If the tip is approximated as a sphere, the spectral density of the transverse field near the tip's axis is $S_{B_x} = S_{m_x} B_{\text{tip}}^2 / 4m_{\text{tip}}^2$, yielding the relaxation rate,

$$\frac{1}{T_1} = \frac{\alpha \gamma_s^2 B_{\text{tip}}^2 k_B T}{2 \gamma_m B_A^2 m_{\text{tip}}}. \quad (2)$$

Note that the relaxation rate depends strongly on magnetic anisotropy, in qualitative agreement with numerical simulations [23]. Using the parameters for our tip and assuming $\alpha = 0.1$, $\gamma_m \approx \gamma_s$, and $B_{\text{tip}} = 75$ mT (equivalent to $d_{\text{slice}} = 800$ nm), we find $T_1 = 5 \times 10^5$ s.

Since this T_1 is orders of magnitude longer than that observed experimentally, we conclude that magnetic fluctuations originating from the volume of the tip are not a factor in the tip-induced relaxation. However, this conclusion is based on an idealized tip with very high anisotropy. Since the tip surface has undoubtedly been damaged by ion milling and oxidation, the surface likely has reduced anisotropy and therefore contributes some additional field noise. We also note that, even for an idealized tip, tip-induced relaxation can be expected to increase dramatically as the geometry is scaled down in size since, for a fixed value of B_{tip} , the relaxation rate scales inversely with the tip moment (i.e., tip volume).

Another important source of magnetic noise is due to thermal currents in the electrically conductive tip. This noise source, which is present even when the tip is nonmagnetic, has been analyzed previously in the context of biomagnetic measurements [25] and spin relaxation [26]. For most geometries, expressions for the magnetic noise are complicated. But, for the case of a thin nonmagnetic slab, an analytical expression is available: $S_{B_x} = (\mu_0^2 \sigma k_B T / 32\pi) [t/d(d+t)]$, where d is the distance from the slab, t is the slab thickness, and σ is the conductivity [25,26]. This equation is valid for slab thicknesses thin compared to the skin depth $(2/\mu_0 \sigma \omega_0)^{1/2}$. If we roughly approximate the tip as a thin slab, then the relaxation rate is

$$\frac{1}{T_1} = \frac{\gamma_s^2 \mu_0^2 \sigma t k_B T}{32\pi d_{\text{slice}} (d_{\text{slice}} + t)}. \quad (3)$$

For $\sigma = 10^7 \Omega^{-1} \text{ m}^{-1}$ (characteristic of an alloy at low temperature) and $t \approx d_{\text{slice}} \approx 1 \mu\text{m}$ (characteristic of the tip size and spacing), Eq. (3) yields $T_1 = 10$ s. Thus, the relaxation rate due to thermal currents is significant and of the same order of magnitude as the observed effect.

The work presented here represents an initial step towards understanding and ultimately controlling relaxation effects for spins located within submicron proximity of a readout device. Further studies with smaller ferromagnets, closer proximity, and lower temperature are required to see if additional relaxation effects are uncovered and to evaluate the viability of extension to single-spin detection. Although this study has focused on MRFM techniques, many

of the issues considered here are likely to be relevant to other solid-state quantum measurement devices.

We thank P. Rice and C. Rettner for help with tip preparation, L. Folks and R. C. Woodward for the PrFeB material, T. P. Seward for the silica, P. Kasai for spin concentration measurements, and J. A. Sidles for insightful discussions regarding relaxation mechanisms. This work was partially supported by the Office of Naval Research and the NSF-GOALI program.

-
- [1] S. Lloyd, *Science* **261**, 1569 (1993).
 - [2] D. P. DiVincenzo, *Science* **270**, 255 (1995).
 - [3] B. E. Kane, *Nature (London)* **393**, 133 (1998).
 - [4] D. D. Awschalom and J. M. Kikkawa, *Phys. Today* **48**, 33 (1999).
 - [5] J. A. Sidles, *Phys. Rev. Lett.* **68**, 1124 (1992).
 - [6] J. A. Sidles *et al.*, *Rev. Mod. Phys.* **67**, 249 (1995).
 - [7] D. Rugar, C. S. Yannoni, and J. A. Sidles, *Nature (London)* **360**, 563 (1992).
 - [8] D. Rugar *et al.*, *Science* **264**, 1560 (1994).
 - [9] Z. Zhang, P. C. Hammel, and P. E. Wigen, *Appl. Phys. Lett.* **68**, 2005 (1996).
 - [10] G. M. Leskowitz, L. A. Madsen, and D. P. Weitekamp, *Solid State Nucl. Magn. Reson.* **11**, 73 (1998).
 - [11] K. J. Bruland *et al.*, *Appl. Phys. Lett.* **73**, 3159 (1998).
 - [12] W. M. Dougherty *et al.*, *J. Magn. Reson.* **143**, 106 (2000).
 - [13] B. C. Stipe *et al.*, *Phys. Rev. Lett.* **87**, 96801 (2001).
 - [14] D. Rugar, H. J. Mamin, and P. Guethner, *Appl. Phys. Lett.* **55**, 2588 (1989).
 - [15] R. A. Weeks and C. M. Nelson, *J. Appl. Phys.* **31**, 1555 (1960).
 - [16] J. G. Castle, Jr. and D. W. Feldman, *J. Appl. Phys.* **36**, 124 (1965).
 - [17] K. Wago, D. Botkin, C. S. Yannoni, and D. Rugar, *Phys. Rev. B* **57**, 1108 (1998).
 - [18] B. C. Stipe *et al.*, *Phys. Rev. Lett.* **86**, 2874 (2001).
 - [19] S. Hirose *et al.*, *J. Appl. Phys.* **59**, 873 (1986).
 - [20] T. R. Albrecht, P. Grütter, D. Horne, and D. Rugar, *J. Appl. Phys.* **69**, 668 (1991).
 - [21] The adiabatic reversal was alternately started at opposite extremes of the cantilever motion. The spin motion was thus locked either in phase or antiphase with respect to the cantilever motion, leading to opposite cantilever frequency shift. A difference was then taken to eliminate any common-mode (nonspin) response. For the T_1 measurements, low frequency ($1/f$) noise was further suppressed by employing a modulation technique wherein the B_1 field was turned off for one-half cantilever period every 256 cantilever cycles. This has the effect of flipping the phase of the spin reversals by 180° , leading to a signal oscillating at $f_c/512 \approx 42$ Hz. This signal was detected using a synchronous detection (lock-in) scheme.
 - [22] C. P. Slichter, *Principles of Magnetic Resonance* (Springer-Verlag, Berlin, 1990), p. 209.
 - [23] J. D. Hannay, R. W. Chantrell, and D. Rugar, *J. Appl. Phys.* **87**, 6827 (2000).
 - [24] N. Smith and P. Arnett, *Appl. Phys. Lett.* **78**, 1448 (2001).
 - [25] T. Varpula and T. Poutanen, *J. Appl. Phys.* **55**, 4015 (1984).
 - [26] J. A. Sidles, quant-ph/0004106 (<http://xxx.lanl.gov>).